Properties of Montmorillonite-Containing Natural Rubber

B. Jurkowska,[1] B. Jurkowski,[2] M. Oczkowski,[1,2] S. S. Pesetskii,[3] V. Koval,[3] Y. A. Olkhov[4]

[1]*Research and Development Center of the Tire Industry (OBR PO) Stomil, 61-361 Poznan, Starolecka 18, Poland*
[2]*Plastic and Rubber Processing Division, Institute of Materials Technology, Poznan University of Technology, Piotrowo 3, 60-950 Poznan, Poland*
[3]*V.A. Belyi Metal-Polymer Research Institute (MPRI), National Academy of Sciences, 32a Kirov Street, Gomel, 246652, Republic of Belarus*
[4]*Institute of the Problems of Chemical Physics, Russian Academy of Sciences, 142 432 Chernogolovka, Moscow Region, Russia*

Received 7 September 2006; accepted 29 March 2007
DOI 10.1002/app.26657
Published online 19 June 2007 in Wiley InterScience (www.interscience.wiley.com).

ABSTRACT: A melt compounding process was used to prepare hybrid nanocomposites based on natural rubber (NR) and montmorillonite (MMT) modified with octadecylamine. Cured rubber was subjected to complex testing. Most likely modified MMT participates in physical networking of a low-temperature topological region (soft amorphous fraction) of NR networked by low energy junctions. There was a significant difference between behavior of NR containing modified and neat montmorillonite and also those measured at low strain (5–50%) and above 150–170%. Because of this, to optimize compounding process of nanocomposite it is necessary to apply properties those determined under conditions as much as possible close to the usage conditions. © 2007 Wiley Periodicals, Inc. J Appl Polym Sci 106: 360–371, 2007

Key words: nanocomposite; rubber; NR; montmorillonite; mechanical properties; TMA; DMA

INTRODUCTION

Filler particle size and its distribution, structure, and length/diameter ratio have a large influence on the physical performance of the composite. Rubbers are usually filled with carbon black or silica to improve the mechanical properties. Carbon black is an efficient reinforcement because of its strong interaction with carbon-chain rubber, but at high loading, it decreases the processability of rubber compounds. One of alternative fillers for rubber and plastics[1–5] is montmorillonite (MMT), but because of large size of particles and low surface activity, its reinforcing capacity is poor. To change this situation, the MMT-organic interactions are studied for years[6–8] to make possible manufacturing of polymer nanocomposites with new properties.[9,10] It is because MMT is composed of silicate layers 1 nm thick and about 0.2–2 μm in other directions.[6,11–13] Its structure contains one octahedral between two tetrahedral layers.[13] Weak intermolecular (van der Waals) forces occur between them.[14] For that reason, their internal and external cations can be exchanged by other ions giving organomodified MMT.[14–16] The organic cations decrease the surface energy of MMT and makes intercalation possible. Exfoliated MMT further enhances the properties related to the intercalated ones.[8] This makes possible the silicate to be dispersed at compounding and more compatible and, as a result, be effective reinforcement for natural rubber (NR),[5,8,9,17–21] polyamide,[22,23] polypropylene,[24,25] polystyrene,[26] and polycarbonate.[27] Interestingly, significant improvements in variety of properties (mechanical, barrier, flame retardancy) could be achieved at low loading.[27–29,30] According to[9,31] 15 phr of MMT gives optimum tensile and tear properties of rubbers comparable to those loaded with 40 phr of carbon black. However, considering economical viewpoint, now it is rather difficult to introduce MMT into industrial application.

Intercalation and exfoliation of MMT in NR matrix is possible by melt mixing,[32] but it is difficult to be achieved.[33,34] In spite of it, an increase in modulus of rubber was observed by many scientists. It suggests that achieved dispersion level, independently on a fact whether is it intercalated or exfoliated structure, improves rubber properties. Investigating an influence of MMT usually some properties of rubbers are tested only what makes difficult to compare conclusions from different publications. Because of this, the main goal of this study is to investigate very different properties and structural characteristics of NR vulcanizates containing a low share of organomodified MMT.

Correspondence to: B. Jurkowski (boleslaw.jurkowski@put.poznan.pl).

Contract grant sponsor: Polish State Committee of Scientific Research; contract grant number: 4 T08E 06725.
Contract grant sponsor: Poznan University of Technology; contract grant number: TB-29-019/2003.

TABLE I
Rubber Formulation

Component		Concentration (phr)				
		*M*0	*M*1	*M*2	*M*3	*F*1
Mixing Stage 1	Natural Rubber (SMR 20)			100		
	ZnO			5.0		
	Stearic acid			2.0		
	Filler					
	Carbon black N220	–	–	–	–	50
	Montmorillonite	–	10	5[a]	10[a]	–
	Dusantox IPPD			1.2		
	Matoflex TMQ			1.5		
Mixing Stage 2	Vulkasil CBS			0.6		
	Duslin PP			0.2		
	Mineral sulfur S95			2.6		

[a] Organomodified montmorillonite (treated with octadecylamine $C_{18}H_{39}N$ and named C18–MMT).

EXPERIMENTAL

Materials

Two rubber compounds (*M*0 without any filler and *F*1 containing 50 phr of carbon black grade N220 (Carbochem Factory, Gliwice, Poland) taken as a reference and three containing MMT were investigated. Namely *M*1 with 10 phr of neat MMT (aluminum hydrosilicate–untreated, FLUKA), *M*2 and *M*3 adequately with 5 and 10 phr MMT treated with octadecylamine ($C_{18}H_{39}N$ for synthesis–MERCK) named C18-MMT were prepared (Table I).

In this study, 50 phr of carbon black or MMT in amount 10 phr and C18-MMT in amount 5 and 10 phr were added to NR (grade SMR 20, Malaysia–100 phr). Modification of MMT was performed following the procedure described below. The other ingredients were supplied: ZnO by Metallurgic Plant, Bedzin, Poland, stearic acid by Nitrogen Plant, Kedzierzyn, Poland, Dusantox IPPD by Duslo-Sala, Slovakia, Matoflex TMQ, Hungary, Vulkasil CBS by Duslo-Sala, Slovakia, Duslin PP by Duslo-Sala, Slovakia, and mineral sulfur by Siarkopol, Tarnobrzeg, Poland. All were standard commercial grade materials.

MMT modification

MMT was dispersed in hot distilled water (about 80°C) by using a propeller mixer working at 600 rpm. Octadecylamine and HCl (concentration 35.5–38%) were dissolved in hot distilled water. Then, the hot water suspension of MMT was poured into this solution and homogenized for about 10 min to yield white precipitate. Next, precipitate was washed with distilled hot water three times, and freeze-dried to yield an organophilic MMT intercalated with octadecylamine. Washes were controlled by addition of $AgNO_3$ until no precipitate of AgCl was formed, to ensure the completed removal of chloride ions. The product (C18-MMT) was dried to constant weight in a vacuum oven at 80°C.

Preparation of rubber compound and vulcanization

Rubber compounds *M*0 and *F*1 were prepared in a laboratory Banbury-type internal mixer (volume 2 l, Meccaniche Moderne, Italy) at 40 rpm. Mixing time was for *M*0–5 min, and for *F*1–7 min.

MMT-containing compounds were prepared on a laboratory open mill (with a friction ratio of 1 : 1.14) in two steps. The compounding procedure for the first step: raw rubber (7 min), additives: ZnO, stearic acid, Santoflex IP, Flectol H (5 min) and, then, neat MMT or C18-MMT (7 min). In the second step of mixing lasting 7 min curatives were added.

The rubber compounds were cured in respective molds in electrically heated press with a table of 400 mm × 400 mm at 150°C for optimum cure time (t_{90}), which was determined from an oscillating disk rheometer (Monsanto R100, St. Luis, MO) and the larger specimens were vulcanized 5 min longer above optimum cure time.

Testing methods

Tensile strength characteristics were measured according to ISO 37 : 1994 and tear resistance according to ISO 34-1 : 1994 (an unnicked 90° angle specimen) both using Instron 4466 Universal Testing Machine (Instron, High Wycombe Bucks, UK) at speed of 100 mm/min. Additionally, the tangent moduli (slope of the stress–strain curve at a given strain) were evaluated.[65] Aging of the specimens was performed according to ISO 188 : 1998 in an air-circulation heating oven (model UT6060, Heraeus Instruments, Hanau, Germany) operated at 70°C for 168 h.

Rebound resilience was measured according to ISO 4662 : 1986 using a tester model 5109.01, Zwick, Germany.

Low speed hysteresis was measured at room temperature (21°C) using an Instron 1115 tensile testing machine (Instron, High Wycombe Bucks, UK). Loading was performed in 10 cycles running from zero to 1.2 MPa and back to zero at a compression rate of 10 mm/min. Hysteresis loss was measured by subtracting the area under the force-retraction curve from the area under force-deformation curve. Low speed hysteresis was calculated as the ratio of hysteresis loss to the area under the force-deformation curve.

Temperature rise and compression set (permanent deformation) were tested by a Goodrich-type flexometer (model FR-2, Metallist, Leningrad, Russia) in which the specimen was compressed at a frequency of 30 Hz at both room temperature and 40°C.

Hardness (Shore A) was measured using a tester KABID–PRESS KP 15004, Poland.

The wetting angle of the specimens by distilled water and medical Vaseline Oil (VO) has been measured by special device developed at Metal-Polymer Research Institute–MPRI, Gomel, Belarus. The specimen decreased by alcohol was placed on the movable table and about 40 mm^3 drop of a standard liquid was put on its surface from a syringe. After 1 min, the wetting angle was computer-recorded from the image of the drop obtained by a long-focus microscope.

A tribometer (producer MPRI, Belarus) with a steel spherical indenter 3 mm in diameter that reciprocating over a 5 mm long friction path was used for triboengineering testing. The friction coefficient μ was measured under 0.2 and 0.5*N* loads on the indents.

Infrared spectral analysis was done on the FTIR spectrometer (model Bruker ISS 113v, Germany) on wave number range 4000–400 cm^{-1}.

The inorganic content of C18-MMT was measured by weighting before and after burning out of its organic parts.

Electro-physical properties as relative permittivity (ε) and the tangent of dielectric loss angle (tan δ) of the specimens were measured according to the Russian State Standard 6433.4-71 using industrial frequency currents (50 Hz). A typical device for thermostimulated depolarization of dielectrics recorded the spectra of thermally stimulated currents (TSC) of the specimens. To characterize a relative permittivity ε tan δ, conductance G_E, superficial resistance R_E the AC-DC LCR circuit was used. The results are averaged from 5 to 7 replicate measurement.

The coefficients of reflection *R* and attenuation *S* of the electromagnetic radiation passing through the specimens under study were estimated. For it, the scatterometric method and a panoramic indicator (model P2-61, Russia) were used to measure the standing-wave factor by the voltage (SWFv). The specimens were placed into a wave-guide path of the indicator and tested under a normal incidence of the electromagnetic wave (EMW) within 8 till 12 GHz frequency range ν (wavelengths λ = 3.75–2.5 cm). To estimate the reflection coefficient, the specimens were brought into contact with a metal substrate that reflecting the radiation and placed into the wave-guide path of the indicator, where the SWFv was measured at different ν. The reflection coefficients was calculated by the formula $R = (\text{SWFv}-1) \times 100/(\text{SWFv} + 1)$, %.

The dynamic G-moduli and related tan δ were determined by using an inverse torsion pendulum device (DMA) designed at MPRI.[35–37] The specimens in the form of strips 50 mm × 5 mm × 0.5 mm in size were heated over the temperature range from –150 up to 200°C at a rate of 1.5°C/min. The temperatures were measured within ±0.1°C accuracy. The pendulum twist angle was 3° and the oscillation frequency was 1 ± 0.01 Hz. Deviations in G-modulus measurements were 3–5%.

The UIP-70M apparatus (Central Design Bureau of the Russian Academy of Sciences, Moscow, Russia) was used for thermomechanical analysis (TMA). The procedure is as follows: the specimen was put into the measuring cell of the thermostatic chamber. It was frozen without pressing under a scanning rate of 4°C/min, starting from room temperature, usually to –120°C. Next, the specimen was stored for 10–15 min to equalize a thermal field within it. To obtain the thermomechanical curve (TMC), the probe with a stable, but small load is moved down to contact the surface of the specimen and the material is heated.

The TMA allows[38,39] to determine temperatures of the glass transition T_g and the beginning of flow T_f. It is possible to identify several regions in a surface layer of the tested polymer material characterized by three physical states each and differing in linear thermal expansion coefficients in glassy and rubbery states.[38,39] TMA also makes possible to evaluate the molecular-weight characteristic for the chain segments between junctions in individual regions. Simultaneously, evaluation of the compaction factor $V_c^{\text{TMA}} \approx 3(\alpha_1 - \alpha_2)T_g$ could be done,[39–41] where α_1 is the coefficient of linear thermal expansion in a glassy state = $(\Delta H/H_o)/\Delta T$, where $\Delta H/H_o$ is a relative change in the initial height H_o (specimen thickness) within the temperature interval, ΔT, α_2—as α_1 but in a rubbery state. However, usability of these characteristics for optimizing the composite formulation and processing parameters is limited due to several factors: First, TMA tests a surface layer up to 0.5 mm thick[42] when in mechanical measurements a specimen is usually much thicker depending on

which test is considered. This fact influences the gradient of all crosslink density of specimen, crystallinity degree and crystals' sizes distribution while the material is crystallizable. Second are the testing conditions, and third is the material state when testing (bulk or dissolved). In spite of it, several mechanical characteristics of rubber correlate with those from the TMA.[43]

RESULTS AND DISCUSSION

Mechanical properties

NR compounds filled with C18-MMT show faster vulcanization with respect to that of neat MMT. The rubbers containing both neat and modified MMT were soft and very elastic due to low filling degree. However, addition of C18-MMT (5 and 10 phr) changes significantly mechanical properties of NR cured rubber (Table II).

The specimens were extended up to 300% only. The increase in stress at 100, 200, and 300% strain of specimen containing C18-MMT in comparison to the case of neat MMT was observed. It could be resulted from the increase in the effective crosslink density of the rubber network (Table III) as it was discussed in literature.[8] Between specimens *M*1 and *M*3 with the same concentration of MMT unmodified and modified, the difference in stiffness was twice as large. The highest stiffness at strain was observed for the reference rubber containing 50 phr of carbon black (*F*1).

Tangent modulus (slope of the stress–strain curve), at strain not exceeding 20–30% correlates with properties of rubber goods at usage.[44–46] Because of this, it is useful for computer simulation of stress distribution in rubber items. Simultaneously, at low strain is more visible effect of filler reinforcing and are low the effects dependent on orientation of the chain segments between junctions of the rubber network and pseudo-network, especially phenomena related with strain–induced crystallization observed at higher strain and crystallites rearrangement at cyclic loading when substantial influence has temperature often changing at test. Value of tangent modulus increases as concentration of modified MMT grows (Figure 1). This fact suggests that at testing are degraded both rubber/filler junctions of different energies and junctions between MMT platelets within not dispersed MMT agglomerates, if present. These junctions of rubber pseudo-network could influence rubber stiffness, strength, and dissipation of energy at deformation.

Simultaneously one should consider that stress determined at 100% strain has a magnitude higher than tangent modulus (Figure 1). The latter fact is related to effects dependent on orientation of the polymer chain segments between junctions of the rubber network and pseudo-network (including clusters, nano- and micro-crystalites formation, if present) and relaxation processes all influencing the shape of strain–stress curves for filled rubbers. These ordered small formations act as additional junctions in the network, amplifiers of local strain, and to some extent [8]as filler particles. One would expect the

TABLE II
Mechanical and Electrical Properties of Cured Rubbers

Properties		Filler concentration (specimens) (phr)				
		0 (*M*0)	5[a] (*M*2)	10[a] (*M*3)	10 (*M*1)	50[b] (*F*1)
Before aging	Hardness [Shore A]	23.8 ± 0.3	38.2 ± 07	40.3 ± 0.6	28.2 ± 0.7	59.5 ± 0.4
	Stress at 100% strain (MPa)	0.7 ± 0.07	1.1 ± 0.07	1.4 ± 0.1	0.7 ± 0.03	3.1 ± 0.16
	Stress at 200% strain (MPa)	1.2 ± 0.13	1.9 ± 0.08	2.4 ± 0.18	1.1 ± 0.01	6.8 ± 0.36
	Stress at 300% strain (MPa)	1.8 ± 0.25	2.9 ± 0.09	3.6 ± 0.35	1.6 ± 0.03	11.3 ± 0.63
After aging	Hardness [Shore A]	32.7 ± 0.6	43.7 ± 0.5	47.5 ± 1.3	36.7 ± 0.6	65.0 ± 1.2
	Stress at 100% strain (MPa)	0.7 ± 0.45	1.3 ± 0.07	1.5 ± 0.12	0.8 ± 0.11	4.2 ± 0.07
	$M_{ag}100/M100$	1.00	1.18	1.07	1.14	1.35
	Stress at 200% strain (MPa)	1.2 ± 0.50	2.3 ± 0.14	2.6 ± 0.13	1.4 ± 0.17	9.5 ± 0.21
	$M_{ag}200/M200$	1.00	1.21	1.08	1.27	1.40
	Stress at 300% strain (MPa)	1.9 ± 0.60	3.7 ± 0.24	4.1 ± 0.13	2.1 ± 0.28	15.1 ± 0.25
	$M_{ag}300/M300$	1.06	1.28	1.14	1.31	1.34
Wetting	By water[c]	77.0	92.0	88.0	93.0	83.5
angles Θ, degrees	By oil[d]	19.5	14.0	15.0	17.0	16.0
Relative permittivity ϵ		5.7 ± 0.1	5.7 ± 0.1	5.6 ± 0.1	6.2 ± 0.1	4.9 ± 0.1
Tangent of dielectric loss angle		0.5 ± 0.02	0.007 ± 0.0002	0.005 ± 0.0002	0.010 ± 0.0002	0.003 ± 0.0002
Conductance G_E (S)		4.9×10^{-6}	$<10^{-10}$	$<10^{-10}$	$<10^{-10}$	8.0×10^{-6}
Superficial resistance R_E (Ω)		3.3×10^{4}	7.7×10^{6}	7.1×10^{6}	6.7×10^{6}	1.05×10^{6}

[a] Rubbers with C18–MMT.
[b] Rubbers with carbon black N220.
[c] Measurements error ± 4.8%.
[d] Measurements error ± 11%.
M_{ag}/M is a ratio of stress after aging to that initial ones for respective strains.

TABLE III
Characteristics of Molecular and Topological Structures of Rubbers

Analyzed parameter[a] (95% confidence limit)	Filler concentration, phr (specimens)				
	0 (*M*0)	5[b] (*M*2)	10[b] (*M*3)	10 (*M*1)	50[c] (*F*1)
Low-temperature Amorphous Region					
T_g,°C (±3 − 5)	−71	−69	−69	−67	−77
$\alpha_1 \times 10^5$ deg^{-1} (±10%)	6.9	5.85	9.42	5.45	8.7
$\alpha_2 \times 10^5$ deg^{-1} (±10%)	26.1	28.6	29.6	21.5	25.8
$\alpha_2\alpha_1$	3.78	4.89	3.14	3.94	2.97
V_c^{TMA} (±10%)	0.116	0.139	0.124	0.099	0.101
$\bar{M}'_{n(n)} \times 10^{-3}$ g/mol (±10%)	8.87	4.49	3.03	6.12	1.32
$\bar{M}'_{n(w)} \times 10^{-3}$ g/mol (±10%)	17.23	7.26	4.13	9.19	2.51
K' (±10%)	1.94	1.62	1.36	1.5	1.91
T'_∞,°C (±3 − 5)	95	22	−31	−5	108
φ' (±10%)	1	0.53	0.38	0.44	0.29
High-temperature Amorphous Region					
T_{htt},°C (± 3 − 5)	–	107	130	116	108
$\alpha_3 \times 10^5$ deg^{-1} (±10%)	–	−333.3	−111.1	−176.5	−666.0
$\bar{M}''_{n(n)} \times 10^{-3}$ g/mol (±10%)	–	6.76	12.25	17.42	8.41
$\bar{M}''_{n(w)} \times 10^{-3}$ g/mol (±10%)	–	9.44	16.65	23.91	11.59
K'' (±10%)	–	1.4	1.36	1.37	1.38
T''_∞,°C (±3 − 5)	–	195	207	199	198
φ'' (±10%)	–	0.47	0.62	0.56	0.71
T_f,°C (±3 − 5)	–	236	228	206	241
Values Averaged Over Regions					
$\bar{M}_{n(n)} \times 10^{-3}$ g/mol (±10%)	–	5.32	5.68	9.62	3.29
K (±10%)	–	1.56	2.09	1.81	2.72

[a] T_g is temperature of the glass transition, T_f is temperature of the beginning of molecular flow, T_∞ is temperature of the beginning of the plateau of high-elasticity, T_{htt} is temperature of the high-temperature transition, α_1 is coefficient of linear thermal expansion in a glassy state, α_2–as α_1 but in a rubbery state, V_c^{TMA} is compaction factor, α_3 is the coefficient of linear thermal expansion of in a rubbery state, intermediate-temperature region, φ is a share of amorphous region, K is the polydispersity index, $\bar{M}_{n(n)}$is the number-average molecular weight, $\bar{M}_{n(w)}$is the weight-average molecular weight.
[b] Rubbers with C18–MMT.
[c] Rubbers with carbon black N220.

intercalated rubber chains (possible to be present at our experimental conditions[32]) to be in a more extended conformation than those outside the MMT galleries, thus favoring the crystallization process.[8] The introduction of filler causes[47] that the lateral crystallite size of NR decreases, but increases the fluctuation of rubber chains orientation. Simultaneously, rubber stiffness depends on limited extensibility of the short chain segments bridging neighboring MMT particles[48,49] if filler is uniformly dispersed within a polymer matrix or this extensibility is reduced only a little if the physical junctions are gathered and the hindered[32] strain-induced crystallization. The first case is characteristic for multimodal MWD between the network junctions. In addition, the rate of stiffness increase both before and after aging depends on strain at which stress was measured. All these evidence that modified MMT participates in physical networking of rubber. However,[30] a presence of the nonexfoliated MMT layers in NR vulcanizates found by X-ray diffraction, but not found by TEM, evidences that by using the melt-mixing of NR, even supported by previous co-coagulation of latex and MMT aqueous suspension, it is very difficult to ensure MMT exfoliation.

In the stress–strain curve could be discriminated[50–64] two zones: First, at very low strain, angle of the curve is steep and is mainly determined by the filler activity. Next, at 15–20% and higher strain, the second zone of stress is mainly determined by a quantity of the filler. Because of this, dependency of tangent modulus also goes through minimum

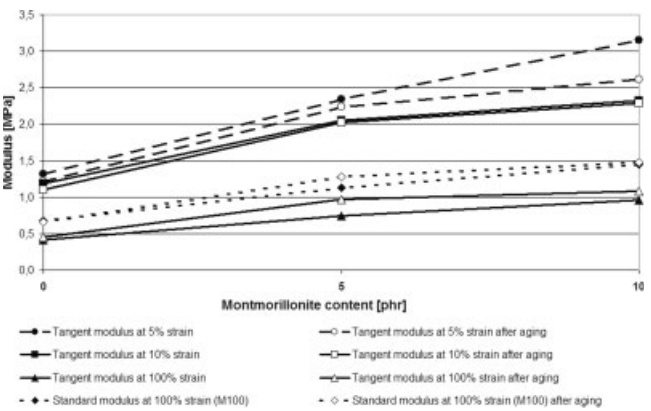

Figure 1 The dependency of tangent modulus at 5, 10, and 100% strain and standard modulus at 100% strain on montmorillonite concentration before and after aging.

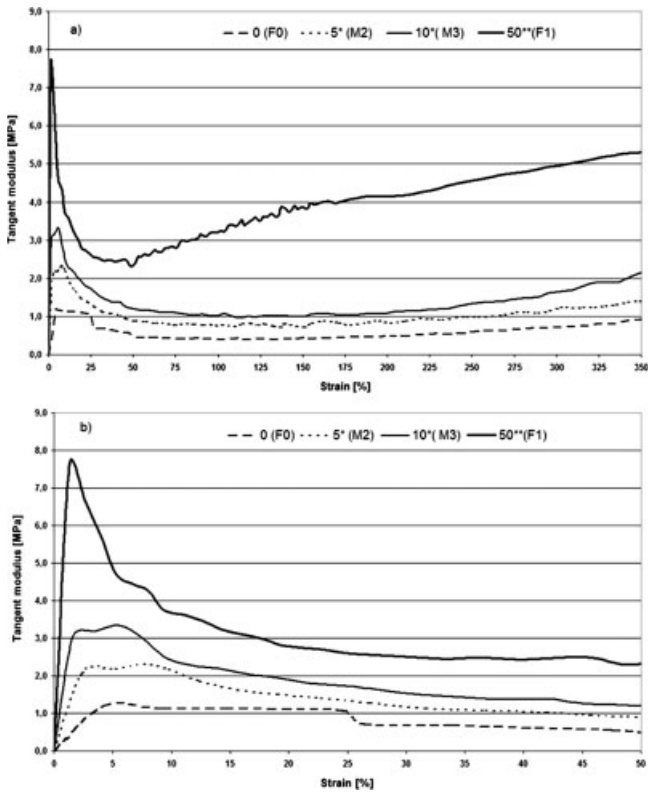

Figure 2 The tangent modulus versus strain for cured natural rubber (a) in all investigated strain range, and (b) the same data but only up to 50% strain.

[Fig. 2(a)]. At low strain (between 3–7% and 50%) it lowers as strain increases while for higher strain (above 50% for carbon-black-filled rubbers and 150–170% for MMT-filled rubbers) it increases. From the above results we conclude that at service conditions, when strains are usually below 20%, the mixed mechanism of degradation of the rubber physical network could be accepted. This phenomenon could not be related with strain-induced crystallization[50] because for such process to appear it is needed[50,51] strain 350% and higher. For gum rubber (*F*0) [Fig. 2(b)] virtually constant magnitude of this modulus is between 4 and 25% strain. Next, a sharp decrease of tangent modulus evidencing degradation of the physical networking junctions was observed. Later, further reduction of modulus was slow or even modulus was preserved constant. This fact evidences that weak and ease rearranging physical networking junctions present in rubber degrade at low strain of carbon-black-filled[52–54] and MMT-filled rubbers.[8] This effect originates from the degradation of filler/filler junctions in the case of highly polar filler or via immobilized layers on the filler surface in the case of strong rubber/filler junctions. This process reduces the stress until about 10% of strain,[55] what results from lowering of the network density at testing conditions.

During compounding it is reasonable to assume that filler, curatives and remaining ingredients are in first approximation uniformly distributed in a rubber matrix and physical pseudo-network is created. During vulcanization a chance to crosslink the neighboring chains is higher in the near of these physical junctions because the chain segments are there in small distance and have reduced mobility. This explains a commonly accepted gathering of cross-links. However, one can assume that only a part of physical junctions participate in gathering of cross-links. The remaining is randomly distributed along the chains. From this it could be concluded that in filled rubber one can expect a presence of differently distributed hybrid physical/chemical and physical junctions of various degradation energies. In our case, when NR is filled with MMT [Fig. 2(a)] for strain >170%, when rubber chains are substantially extended, in the NR network it could be created the stress induced ordered zones (usually smaller than crystallites) acting as additional physical cluster-type junctions reinforcing cross-links creating hybrid structure of the rubber network similar to that described[50] what increases tangent modulus.

Comparing behavior of rubbers with different fillers [Fig. 2(a)] it is visible that 10 phr of C18-MMT gives maximal tangent modulus of 3.0–3.5 MPa, while 50 phr of carbon black gives 7.8 MPa. From this one can assume that to increase rubber stiffness at usage conditions it is reasonable to use MMT only if its price will be reduced.

Accelerated aging causes an increase in rubber stiffness, but a rate of its change is lower for higher content of modified MMT. The rate of changes in stiffness resulted from accelerated aging M_{ag}/M (Table II) especially at 10 phr C18-MMT confirms studies[30] that this filler reduces effects of rubber degradation or additional networking those prevail degradation of the NR network.

Increase in rebound resilience and simultaneous increase in hardness of rubbers containing C18-MMT in comparison to gum rubber *M*0 was noticed (Fig. 3). In case of rebound resilience, the inverse tendency if compare to rubber with 50 phr of carbon black (*F*1) was observed. This situation was expected by analogy to a case when carbon black causes an increase in effective crosslink density of the rubber network due to creating additional physical junctions. Even addition of 10 phr of C18-MMT does not influence on tear resistance (Fig. 4), what could be caused by two phenomena giving opposite results: increase in the network density and some tendency to agglomerate such filler what increases the local stress concentration. Adding C18-MMT reduced a low speed hysteresis in comparison to rubber with neat MMT (*M*1) and to gum rubber (*M*0).

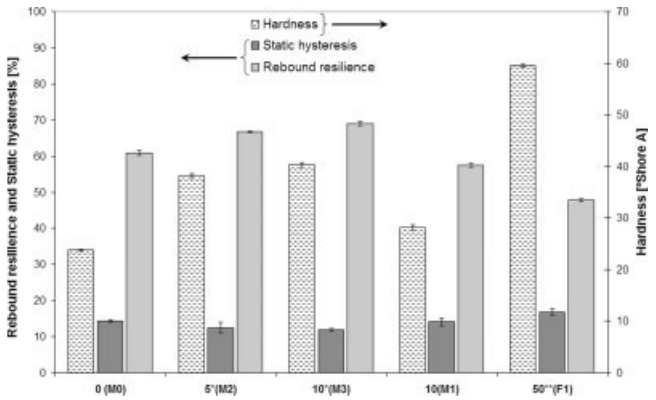

Figure 3 Rebound resilience, hardness, and static hysteresis for rubbers differing in formulation.

The reasons for rubber hysteresis are some changes in its structure at loading. Additionally to degradation of crosslinks and physical junctions in the rubber phase, the permanent transformations (degradation and restoration) of the physical junctions within agglomerates of the filler and on the rubber/filler interface take place.[56] This causes a softening of cured rubber[57] and is reflected in variation of a shape of strain–stress curves during loading and unloading of a specimen during first and successive cycles. It also causes some movement of structural elements changing a size of specimen, called a permanent set. Dynamic test on Goodrich flexometer (Fig. 5) shows a decrease of the permanent set and heat generation giving temperature rise of specimens with C18-MMT. Rubbers became fatigue-resistant. For neat MMT (*M*1) it is different; now filled rubber behaves as cured gum rubber (*M*0) as expected. This evidences that physical branching junctions in the rubber network created by C18-MMT are stronger and are not easy degradable at testing conditions.

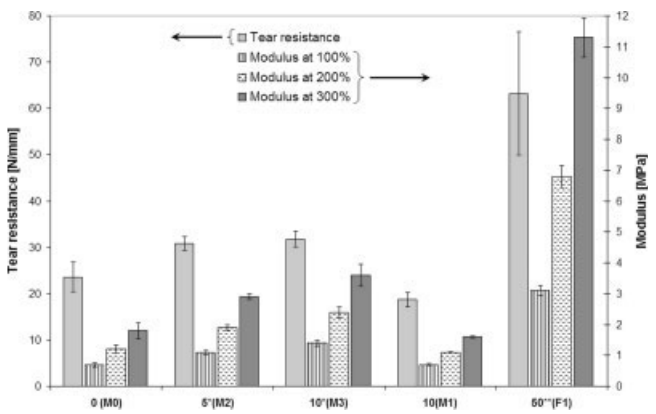

Figure 4 Dependency of tear resistance and modulus at different strain for rubbers differing in formulation.

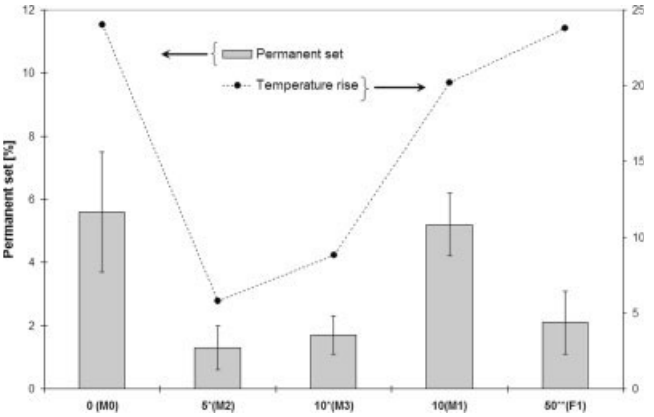

Figure 5 Permanent set and temperature rise determined by dynamic test on Goodrich flexometer for rubbers differing in formulation.

Surface investigations

Wetting characteristics of a rubber surface influence the friction-related phenomena at service conditions. To study some of them, the wetting angle Θ of the cured rubber by distilled water and medical VO has been measured. The results averaged from 5 to 7 replicate measurements are presented in Table II. Rubber wetting by water improves for the specimens containing neat MMT (*M*1), which is hydrophilic—wetting angle increases from 77 to 93°. Introduction of organophilic CM18-MMT (*M*2 and *M*3) causes some increase of rubber wetting angle what is understandable. Wetting of the specimens by VO lowers for both neat MMT and C18-MMT what suggest that influence of the mold release agent remaining after cleaning a rubber surface by acetone is higher than that by fillers investigated.

At triboengineering test almost all recorded curves of coefficient of friction μ(τ) versus time are coincident. Only one specimen filled with the neat MMT (*M* 1) having the minimal μ at load $p = 0.5N$ can be singled out (Fig. 6). This suggests that fillers investigated at given here concentration virtually does no influence on triboengineering properties.

Electrical investigations

Magnitudes of relative permittivity ε and tan δ of the rubbers filled with MMT vary within the measurement error range. In this case, TSC spectra do not bear any significant information (the charge carrier traps are absent). The distinguishing feature is the appearance of current peaks corresponding to charge relaxation of mechanoelectret formed at the test specimen cut-off. The only *M*3 specimen spectrum showed a characteristic peak at about 80°C. It corresponds, most likely, to heat-induced degradation of some junctions in the modified MMT that is shown in Figure 7.

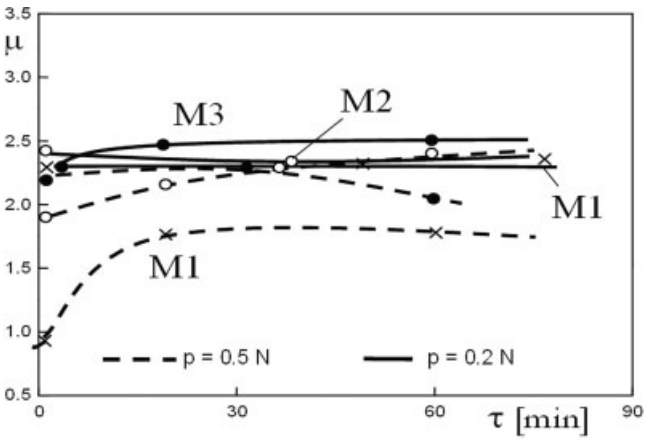

Figure 6 Friction coefficient μ for different loads changing in time.

All the studied rubbers turned to be poor radio absorbing materials (RAM), i.e. their *R*-values are high enough and S is low. Curves $R(\nu)$ and $S(\nu)$ virtually coincide for all the specimens.

Structural investigations

FTIR was carried out to study the effects of functional groups in the C18-MMT with respect to potential interactions with the polymers. On spectrum, there are visible characteristic bands for MMT structure and a band characteristic for octadecylamine (Fig. 8). Peak at wave number 463 cm^{-1} is characteristic for bending vibration of Si–O and peak at wave number 516 cm^{-1}—for tensile vibrations of Al–O.[58] Intensive band at wave number 1032 cm^{-1} is characteristic for MMT tensile vibrations.[3,12,58,59] Insignificant band at wave number 1633 cm^{-1} is ascribed to deformation vibrations of water molecule between MMT platelets' surfaces.[12] Tensile vibration of O–H in MMT is responsible for bands 3628 cm^{-1}.[60] New bands of absorption are visible on C18–MMT spectrum. Namely, band at wave number 1467 cm^{-1} is characteristic for ammonium salt,[12] while 2850 cm^{-1} and 2918 cm^{-1} for symmetric vibration and for

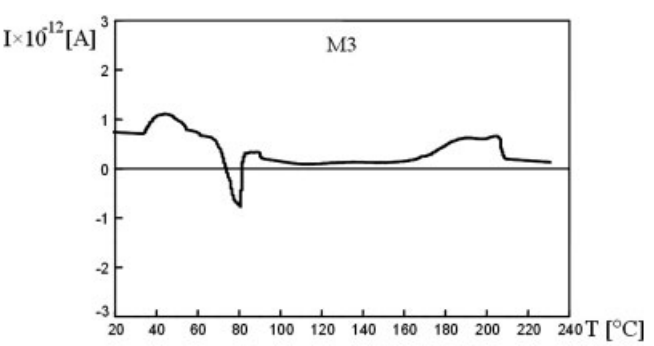

Figure 7 TSC spectra at peak $T \sim 80°C$.

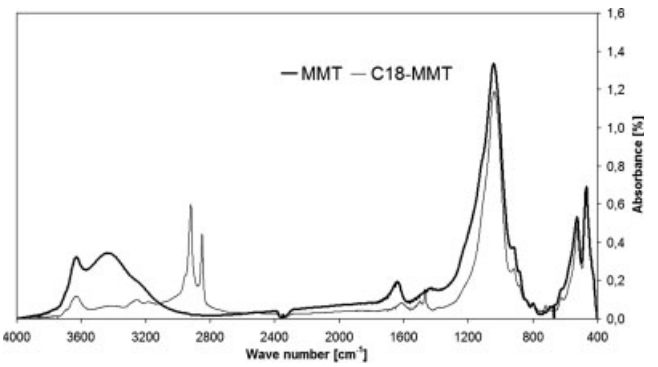

Figure 8 FTIR spectroscopy of modified and neat montmorillonite.

asymmetric aliphatic groups C–H of octadecylamine, adequately.[12] Insignificant band at 3253 cm^{-1} is characteristic for tensile vibration of N–H prime amine. Appearing on spectrum of C18-MMT, the above-mentioned new bands of absorption evidences an exchange of Na cation for ammonium cation.[3] This reaction is also proved by the inorganic content of C18-MMT that was 66.14 wt %.

At temperature range between –150 and –50°C (glassy state of rubber), physical networking and related G-modulus shows some but small influence of the filler used both its surface modification and quantity (Fig. 9). For filling degree 10 phr, modification of MMT increases rubber stiffness measured at −100°C a little from $G = 2.7$ GPa when neat filler used to $G = 2.8$ GPa for modified one. Decrease in the filling degree from 10 to 5 phr of C18-MMT (specimen 2) reduces the G-modulus to 2.5 GPa.

Similar conclusions about physical networking of rubber by this filler could be made while test at higher temperatures, when rubber is in a rubbery state; now the influence of filler is more visible. It means both modification and increased filler content increase G-modulus of rubber significantly (Fig. 10).

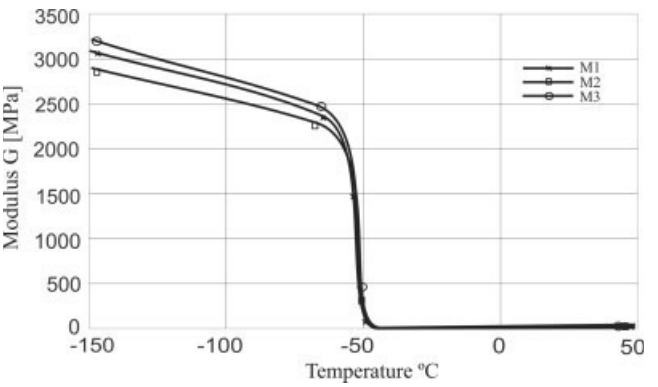

Figure 9 The dependency of G-modulus from DMA test at twisting on montmorillonite content for low-temperature range (standard pendulum).

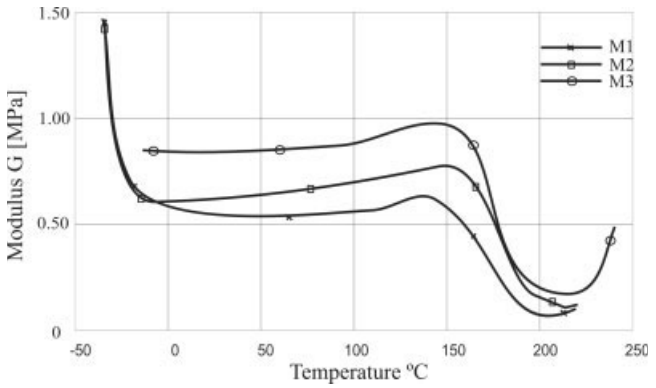

Figure 10 The dependency of G-modulus from DMA test at twisting on montmorillonite content for high-temperature range (lightweight pendulum giving higher sensitivity).

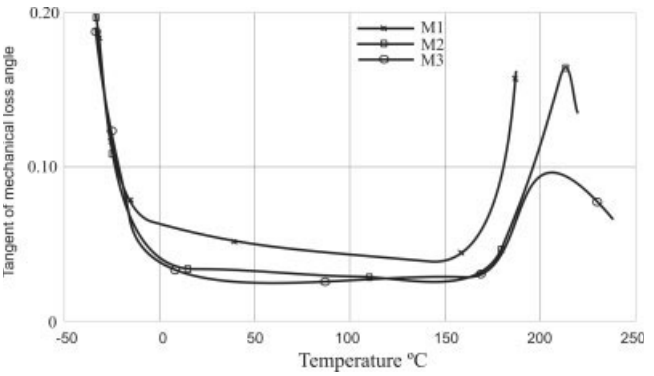

Figure 12 The dependency of tan δ from DMA test at twisting on montmorillonite content for high-temperature range (lightweight pendulum giving higher sensitivity).

This supports previous conclusion concerning stresses at different, but much larger elongations taken from Table II. From this could be concluded that modification of MMT makes specific change in an interaction between its particles and rubber chains. Most likely, modification avoids some agglomeration of MMT particles at melt compounding because it improves compatibility and eases exfoliation[8] with the polymer matrix.

Major peak of tangent of mechanical loss angle (Fig. 11) at the same temperature for all specimens (T_g = –53.2°C) is attributed to the glass transition. It is close to that typical for cured gum NR. The properties evaluated at temperatures between –50 and 250°C (the rubbery state of rubber) seen in Figures 11 and 12 are different from those previously discussed for G-modulus at glassy and rubbery states of rubber.

Small increase or independence (taking into account a scatter of the measured values) of the mechanical loss factor (tan δ) at the glass transition temperature of the rubber with neat MMT if compare with modified are observed (Fig. 11). At 0°C, when rubber is in a rubbery state and measurements are performed by using more sensitive testing regime, the difference is much higher (Fig. 12). The differences in resistance on heat impact are also visible there. Namely, rubber with neat MMT has primary degradation temperature of the network of cured rubber on the level 160–165°C when that for rubber with C18-MMT is higher—on the level 170–175°C. It may be related to large inner friction in the MMT particles and/or agglomerates sheared at test and degradation of low energy rubber/MMT junctions.

It is difficult to discuss a region of tan δ variation above 200°C due to much higher scatter of the measured value there.

The gum rubber is characterized by one topological region determined by TMA. The filled NR has a topological structure with two regions differing in the transition temperatures and thermal expansion coefficients; the filler considerably changes several molecular characteristics of the cured rubber (Table III). This structure is preserved till the high-temperature transition T_{htt} between 107 and 130°C for rubbers containing 5 and 10 phr C18-MMT when begins

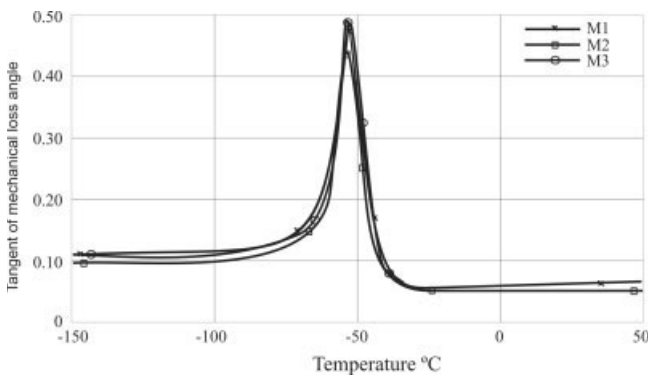

Figure 11 The dependency of tan δ from DMA test at twisting on montmorillonite content for low-temperature range (standard pendulum).

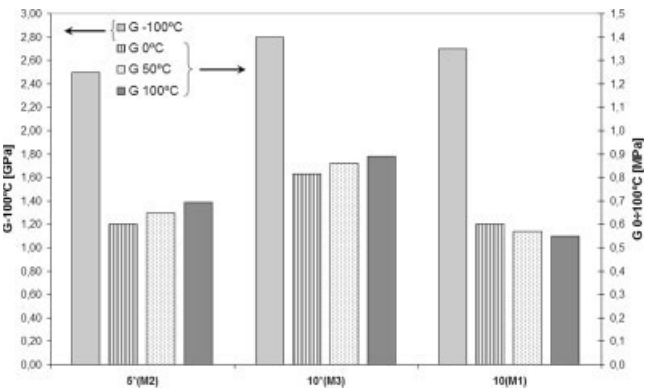

Figure 13 The dependency of G-modulus from DMA test at twisting on montmorillonite content for low-temperature ant high-temperature range.

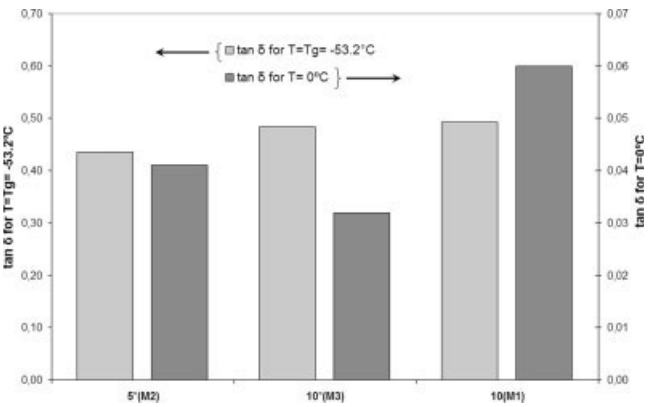

Figure 14 The dependency of tan δ from DMA test at twisting on montmorillonite content for $T = T_g$ and $T = 0°C$.

the thermal degradation of the physical branching junctions of the network of the high-temperature region at testing conditions. This temperature for rubber containing neat MMT is about 116°C and that for carbon-black-filled rubber is 108°C. These junctions are presumably formed by associative structures between neighboring segments of NR with trans-configuration and by interactions of the chain segments with active filler. This degradation process terminates at temperature T''_∞ (about 200°C for all investigated filled rubbers) when begins the rubbery state of the high-temperature region. Its value grows a little as C18-MMT concentration increases. In the low-temperature region different phenomenon is observed, this temperature substantially decreases. For NR containing neat MMT $T'_\infty = -5°C$ when that for carbon-black-filled NR it is 108°C. These data support a well-known fact that nature of filler determines rubber/filler physical interactions. From this experiment, it could be concluded that this additional networking concerns a low-temperature topological region or soft amorphous fraction; it means the most mobile rubber chains or chain segments.

A share of low-temperature region (soft amorphous fraction) lowers and consequently that of high-temperature region (rigid amorphous fraction) grows as concentration of C18-MMT increases. For rubber containing neat MMT it is similar to that containing the same concentration of C18-MMT, but lower than for rubber containing 50 phr of carbon black. It confirms the previous conclusion that shares of topological regions (amorphous fractions) changes in a way dependent on rubber formulation.[61]

The coefficients of linear thermal expansion in a glassy state (α_1) are low dependent on filler concentration within investigated range. On the other hand, α_2, as α_1 but in rubbery state, is correlated with MMT concentration. If $6 > \alpha_2/\alpha_1 \geq 2.5$, it implies preliminarily that the network has the branching junctions of chemical nature. For $\alpha_2/\alpha_1 < 2.5$ the network has junctions of complex (chemical, physical and topological) nature.[62] Values of α_2/α_1 in Table III suggest a chemical nature of the branching junctions. However, it is possible to suppose that in rubbers under investigation strong physical interactions are present; those are comparable in degradation energy with chemical bonds. This structure is not steady[63] and depends on numerous factors, which are yet not investigated in full.

The glass transition temperatures determined by TMA and DMA are different, but both are independent on filler concentration and its kind (Fig. 14 and Table III). The α_2/α_1 ratio of thermal expansion coefficients in rubbery and glassy state is between 2.5 and 5.12 and it is characteristic for amorphous materials.[38,42]

Temperature of the beginning of the plateau of high-elasticity of a low-temperature region, T'_∞, lowers as MMT concentration grows. This agrees with some increase in density of the rubber network (lowering $\overline{M}'_{n(n)}$). The coefficient of polydispersity of rubber chains between the networking junctions is low dependent on a kind of filler investigated.

The compaction factor V_c^{TMA}, a value that is inversely proportional to the volume of all voids within the material, for linear soft-chain polymers in the amorphous state $V_c^{TMA} \approx 0.113$, whereas for rigid-chain polymers, which tend to form the crystalline structures it is below 0.113.[43,63] For polymer composites $V_c^{TMA} \approx 0.113$ implying their less compact structure. In the studied case it has a large dispersion (Table III) caused, most likely, by some heterogeneity of rubber and is in the range typical for composites, but a scatter in its value makes impossible to conclude about influence of MMT kind and its concentration on rubber compactness.

An increase in C18-MMT content is accompanied with the above-mentioned decrease in molecular weight between junctions of a rubber network in a low-temperature topological region and growth in a high-temperature one. It confirms an above-supposed fact that C18-MMT participates in physical networking of a low-temperature topological region (soft amorphous fraction) networked by low energy junctions. Simultaneously, an increase in C18-MMT content is accompanied also with some decrease in temperature of the beginning of flow T_f in comparison with that for carbon-black-filled rubber, but substantial increase in comparison with that for neat MMT. It is known that a polydispersive polymer at this temperature would not flow under the standard processing conditions. For proper processing it is required a higher temperature be reached to ensure a technological flow at a given shear rate, at which the highest MW polymer fractions start to flow. It shows that MMT increases a distance between the neighboring segments of rubber chains, what is evident.

CONCLUSIONS

1. MMT at concentration up to 10 phr virtually does no influence on triboengineering NR properties, but a decrease of the permanent set and heat generation giving temperature rise of specimens with C18-MMT was observed. Adding C18-MMT reduced a low speed hysteresis in comparison to rubber with neat MMT and gum rubber. Rubbers became fatigue-resistant, but poor radio absorbing materials. Increase in rebound resilience and simultaneous increase in hardness in comparison to gum rubber was noticed.
2. Dependency of tangent modulus of rubber on deformation has two parts, namely at relatively low strain (between 5 and 7% and 50%) it lowers as strain increases while for high strain (above 150–170%) it increases. This fact suggests different mechanisms of degradation of the networking junctions of NR vulcanizates containing MMT; this mechanism is dependent on filler concentration. Most likely MMT below 50% strain participates in physical networking of a low-temperature topological region (soft amorphous fraction) of NR that networked by low energy junctions. At high strain (above 150%), when most of the physical junctions are degraded, and rubber chains are substantially extended, in the NR network it could be created the stress induced ordered zones (usually smaller than crystallites) acting as additional physical cluster-type junctions reinforcing cross-links creating a hybrid structure of the rubber network similar to that described[50] what increases tangent modulus.
3. The substantial difference between behaviors of rubber measured at low strain (5–50%) and above 150–170% suggests that for optimization of its formulation and processing it is necessary to apply properties determined under conditions as much as possible close to the usage conditions.
4. Tangent modulus at low strain being a measure of stiffness at usage conditions of most rubber goods is sensitive to addition a small amount of modified MMT.
5. Variations in tensile strength of NR vulcanizates resulted from introduction of modified MMT are small. Because of this, for rubbers compounded by using internal mixers and mixing mills it is hardly to expect that MMT can replace carbon black. However, variations in tensile strength resulted from introduction of modified MMT are smaller than variations in tangent modulus at low strain. It suggests that in rubber specimen still are present areas of stress concentration those reduce strength and/or areas of lower local ordering those reduce physical interactions. From this it could be concluded a need of further study an influence of mixing conditions to improve micro or nanohomogeneity of rubber.

References

1. Alexandre, M.; Dubois, P. Mater Sci Eng 2000, 28, 1.
2. Chen, Y.; Wang, J.; Lin, Y.; Cai, R.; Huang, Z. E. Polymer 2000, 41, 1233.
3. Chow, W. S.; Mohd Ishak, Z. A.; Karger-Kocsis, J.; Apostolov, A. A.; Ishiaku, U. S. Polymer 2003, 44, 7427.
4. Gleiter, H. Acta mater 2000, 48, 1.
5. Okada, A.; Usuki, A.; Kurauchi, T.; Kamigaito, O. C. Y. C.; Bianconi P. A.; Eds. Hybrid Organic–Inorganic Composites. ACS Symp Ser, 1995.
6. Theng, B. K. G. The Chemistry of Clay-Organic Reactions, Wiley: New York, 1974.
7. Greenland, D. J. J Colloid Sci 1963, 18, 647.
8. Joly, S.; Garnaud, G.; Ollitrault, R.; Bokobza, L.; Mark, J. E. Chem Mater 2002, 14, 4202.
9. Ogawa, M.; Kuroda, K. Bull Chem Soc Japan 1997, 70, 2593.
10. Varghese, S.; Karger-Kocsis, J.; Pannikottu, A. Rubber World 2004, 230, 32.
11. Dresselhaus, M. S.; Dresselhaus, G. Nanostructured Mater 1997, 9, 33.
12. Arroyo, M.; López-Manchado, M. A.; Herrero, B. Polymer 2003, 44, 2447.
13. Kühl, A.; Bach, S. Smektite (Bentonite, Montmorillonite) und Hormite (Palygorskit, Sepiolith), Oberseminar, 25.11.99, Available at www.geo.tu-freiberg.de.
14. Beres B. Principles of Mineralogy and Petrography (in Polish), WPW: Wroclaw, 1992.
15. Langaly, G.; Beneke, K. Colloid Polym Sci 1991, 269, 1198.
16. Buckman, H. C.; Brady, N. C. Soil and its Properties (in Polish), PWRiL: Warsaw, 1971.
17. Teh, P. L.; Mohd Ishak, Z. A.; Hashim, A. S.; Karger-Kocsis, J.; Ishiaku, U. S. J Appl Polym Sci 2006, 100, 1083.
18. Burnside, S. D.; Giannelis, E. P. Chem Mater 1995, 7, 1597.
19. Amerogen, G. J. Rubber Chem Technol 1964, 37, 1065.
20. Usuki, A.; Tukigase, A.; Kato, M. Polymer 2002, 43, 2185.
21. Chang, Y.-W.; Yang, Y.; Ryu, S.; Nah, Ch. Polymer Int 2002, 51, 319.
22. Shelley, J. S.; Mather, P. T.; DeVries, K. L. Polymer 2001, 42, 5849.
23. Liu, L.; Qi, Z.; Zhu, X. J Appl Polym Sci 1999, 71, 1133.
24. Reichert, P.; Nitz, H.; Klinke, S.; Brandsch, R.; Thomann, R.; Mulhaupt, R. Macromol Mater Eng 2000, 275, 8.
25. Usuki, A.; Kato, M.; Okada, A.; Kurauchi, T. J Appl Polym Sci 1997 63, 137.
26. Hoffmann, B.; Dietrich, C.; Thomann, R.; Friedrich, C.; Mulhaupt, R. Macromol Rapid Commun 2000, 21, 57.
27. Stretz, H. A.; Koo, J. H.; Dimas, V. M.; Zhang, Y. Polym Prep 2001, 42, 50.
28. Park, C. I.; Park, O. O.; Lim, G. J.; Kim, H. J. Polymer 2001, 42, 7465.
29. Paul, M.; Alexandre, M.; Degee, P.; Henrist, C.; Rulmont, A.; Dubois, P. Polymer 2003, 44, 443.
30. Wang, Y.; Zhang, H.; Wu, Y.; Yang, J.; Zhang, L.; J Appl Polym Sci 2005, 96, 318.
31. Nah, C.; Ryu, H. J.; Han, S. H.; Rhee, J. M.; Lee, M. H. Polym Int 2001, 50, 1265.
32. Wu, Y.; Ma, Y; Wang, Y.; Zhong, L. Macromol Mater Eng 2004, 289, 890.
33. Varghese, S.; Karger-Kocsis, J. J Appl Polym Sci 2004, 9, 813.
34. Arroyo, M.; Lopez-Manchado, M. A.; Herrero, B. Polymer 2003, 44, 2447.

35. Pesetskii, S. S.; Fedorov, V. D.; Jurkowski, B.; Polosmak, N. D. J Appl Polym Sci 1999, 74, 1054.
36. Pesetskii, S. S.; Jurkowski, B.; Koval, V. N.; J Appl Polym Sci 2000, 78, 858.
37. Pesetskii, S. S.; Jurkowski, B.; Storozhuk, I. P.; Koval, V. N. J Appl Polym Sci 1999, 73, 1823.
38. Jurkowski, B.; Jurkowska, B.; Andrzejczak, K. Polymer Test 2002, 21, 135.
39. Olkhov, Y. A.; Jurkowski, B.; J Therm Anal Cal 2005, 81, 489.
40. Boyer, R. F.; Rubber Chem Technol 1963, 36, 1303.
41. Simha, R.; Boyer, R. F. J Chem Phys 1962, 37, 1003.
42. Zielnica, J.; Wasilewicz, P.; Jurkowski, B.; Jurkowska, B. Thermochimica Acta 2004, 414, 255.
43. Jurkowska, B.; Jurkowski, B.; Olkhov, Y. A. J Therm Anal Cal 2005, 81, 27.
44. Komornickii-Kuznecov, V. K.; Radaeva, G. I.; Kucherskii, A. M.; Artiukhina, L. A. Kauchuk i rezina (RU) 1988, 10, 28.
45. Kucherskii, A. M.; Vasilieva, T. N.; Goldberg, B. B. Proizvodstvo shin, RTI i ATI (RU) 1983, 10, 30.
46. Kucherskii, A. M.; Bobylev, G. G.; Goldberg, B. B.; Varaksin, M. E. Kauchuk i rezina (RU) 1984, 10, 29.
47. Poompradub, S.; Tosaka, M.; Kohijiva, S.; Ikeda, Y.; Toki, S.; Sics, I.; Hsiao, B. S. J Appl Physics 2005, 97, 1035.
48. Mark, J. E. J Phys Chem B 2003, 107, 903.
49. Bokobza, L. Polymer 2001, 42, 5415.
50. Toki, S.; Sics, I.; Hsiao, B. S.; Tosaka, M.; Poompradub, S.; Ikeda, Y.; Kohjiya, S. Macromolecules 2005, 38, 7064.
51. Mitchell, G. R.; Polymer 1984, 25, 1562.
52. Payne, A. R. J Appl Polym Sci 1962 6, 57.
53. Payne, A. R. J Appl Polym Sci 1963, 7, 873.
54. Payne, A. R. Rubber J 1964, 146, 36.
55. Kucherskii, A. M. Kauchuk i rezina (RU) 1990, 8, 26.
56. Payne, A. R. J Polym Sci Polym Symp 1974, 48, 169.
57. Mullins, L. J Rubber Res 1947, 16, 275.
58. Qin, H.; Zhao, C.; Zhang, S.; Chen, G.; Yang, M. Polym Degrad Stab 2003, 81, 497.
59. Pramoda, K. P.; Liu, T.; Liu, Z.; He, C.; Sue, H. Polym Degrad Stab 2003, 81, 47.
60. Zhang, W. A.; Chen, D. Z.; Xu, H. Y.; Shen, X. F.; Fang, Y. E. Eu Polym J 2003, 39, 2323.
61. Jurkowski, B.; Jurkowska, B.; Nah, C. Elastomer (Korea) 2002, 37, 234.
62. Olkhov, Y. A.; Gorbushkina, G. A.; Baturin, S. M. RUS. Pat. 1,713,359 A1, 1989.
63. Hill, A. J.; Zipper, M. D.; Tant, M. R.; Stack, G. M.; Jordan, T. C.; Schultz, A. R. J Phys Cond Mat 1996, 8, 3811.
64. Bartenev, G. M.; Kucherskii, A. M. Colloid Zh 1970, 32, 3.
65. Nadolny, K.; Jurkowski B. (under elaboration).